New Journal of Physics
The open-access journal for physics

Enhanced dipole moments in photo-excited TTF–TCNQ dimers

Mina Yoon[1,2,4], **Yoshiyuki Miyamoto**[3] **and Matthias Scheffler**[1]

[1] Fritz-Haber-Institut der Max-Planck-Gesellschaft, Faradayweg 4–6, 14195 Berlin, Germany
[2] Materials Science and Technology Division, Oak Ridge National Laboratory, Oak Ridge, TN 37831, USA
[3] Nanosystem Institute, National Institute of Advanced Industrial Science and Technology (AIST), Central 2, 1-1-1 Umezono, Tsukuba 305-8568, Japan
E-mail: myoon@ornl.gov

New Journal of Physics **13** (2011) 073039 (13pp)
Received 11 January 2011
Published 28 July 2011
Online at http://www.njp.org/
doi:10.1088/1367-2630/13/7/073039

Abstract. We have studied the dynamics of electron transfer between the molecules of an organic donor–acceptor pair upon absorption of light. Specifically, we considered the tetrathiafulvalene (TTF)–7,7,8,8-tetracyanoquinodimethane (TCNQ) donor–acceptor pair using time-dependent density functional theory with local-density approximation. The molecular planes of the two components are parallel to each other, and the optical transition probability is found to be highest when the optical electric field is parallel to these planes. Under these conditions, absorption induces additional electron transfer from TTF to TCNQ in the π-orbitals perpendicular to the molecular plane and, consequently, we found that the dimer's dipole moment perpendicular to the molecular axes is enhanced with the increase rate of 1% in 15 fs. This enhancement reflects the fact that photo-excited electron–hole pairs tend to dissociate, i.e. electrons and holes move away from each other. We thus suggest potential photovoltaic devices employing these molecules as building blocks.

[4] Author to whom any correspondence should be addressed.

Contents

1. Introduction

In recent years, progress in organic electronics has led to the remarkable development of novel devices such as organic light-emitting diodes [1, 2], organic field-effect transistors [3, 4] and organic photovoltaic cells [5–7]. However, these advances were not paralleled by a deeper microscopic understanding of the optical and electronic properties of the building blocks, consisting of organic molecules. For photovoltaic devices, efficiencies in photo-excitation and in subsequent electron–hole (e–h) splitting govern the energy-conversion efficiency. Such an understanding can contribute to further improvements in the performance or lifetime of these devices and first-principles simulation can play a major role for that purpose.

In this paper, we present a theoretical study of the optical properties of tetrathiafulvalene (TTF)–7,7,8,8-tetracyanoquinodimethane (TCNQ) dimers using time-dependent density functional theory (TDDFT). These dimers are electron donor–acceptor pairs, representative of typical materials for organic devices. We found that the pairs display very intriguing electronic effects when optically excited. In particular, the dipolar nature of the dimers changes significantly under optical excitation; the dipole moment of the dimer molecules increases strongly perpendicular to an applied optical field. This is caused by the photo-induced electron transfer from the donor to the acceptor molecule through the molecule's π-orbital, which is oriented normal to the molecular plane. This enhancement reflects the fact that electronically excited e–h pairs tend to dissociate, i.e. electrons and holes move away from each other.

This paper is organized as follows. In section 2, we present our model systems and explain our theoretical approaches. The electronic ground properties of TTF–TCNQ dimers, such as the structural and electronic are discussed in section 3. We focus on the electronic excited stated state properties of the dimer in section 4. Finally, we summarize our results in section 5.

2. Theoretical approach: model systems and computational details

All optical properties presented in this paper were obtained from TDDFT [8] using the first-principles simulation tool for electron–ion dynamics (FPSEID) code [9, 10]. We analyzed

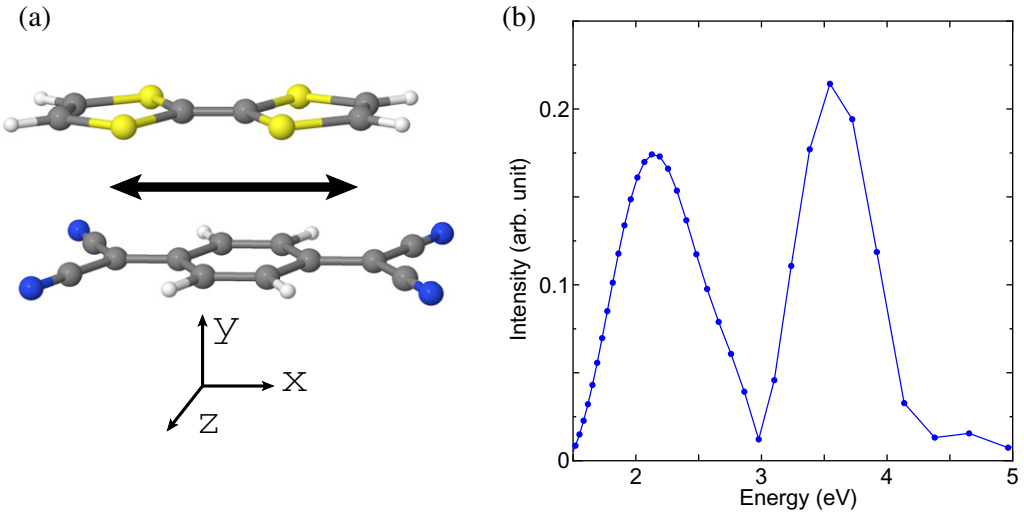

Figure 1. (a) TTF–TCNQ dimer, where an optical electric field is applied in the direction parallel to the molecular axis (indicated by the bold arrow). Atoms are represented by colored spheres; gray is used for C atoms, white for H atoms, yellow for S atoms and blue for N atoms. (b) Calculated optical absorption spectrum with the polarization vector parallel to the arrow shown in (a).

the real-time propagation of electron wave functions while performing molecular dynamics simulations of the ions. We found no noticeable changes in the ionic configurations in our simulation time of 15 fs and thus focused on the electronic dynamics. We used local-density approximation (LDA) [11, 12] of the exchange-correlation (xc) functional. Nuclei plus core electrons are described using the Troullier–Martins pseudopotentials [13], and a plane wave basis was used to describe the valence states. The kinetic energy cutoff was 60 Ry, and sampling in the momentum space is replaced by the Γ-point.

We applied an optical electric field (E-field) to the TTF–TCNQ pair and investigated its structural and electronic properties. The lowest-energy configuration, depicted in figure 1(a), is more stable, by 0.67 eV, than a structure with one of the molecules rotated by 90° in the zx-plane and more stable, by 0.52 eV, than a configuration of TTF/TCNQ interfaces, such as (100) interfaces of TTF and TCNQ bulk. In section 3.1, we compare the structural properties from different theoretical approaches and evaluate the performance of LDA.

In this study, we focus on the e–h dissociation dynamics of the system upon illumination. This is a key event of photovoltaics. Currently, two methods are able to address optical absorption energies based on the DFT. One approach is the GW coupled with the Bethe–Salpeter equation [14] and the other is TDDFT [15–18]. In the GW approach, the excitation is described as the steady limit of response in condensed matter. However, light-induced e–h dissociation phenomena require the description of transient dynamics of photo-excited carriers that can be treated by the real-time propagation of electron wave functions. Thus, we are using here TDDFT to see the transient dynamics of carriers upon photo-excitation. As was suggested by experimental reports on dye molecules [19], for example, the e–h dissociation takes a very short time (typically less than 100 fs), so that conventional perturbation theory that assumes the Fermi-Golden rule at infinite limit of time is not suitable for it. Therefore, in order to describe the light-induced e–h dissociation, the time dependence was considered explicitly. In particular,

we have monitored the time evolution of electron wave functions up to 15 fs. Extending the time scale of our simulation would reveal the evolution of the bound state of e–h pairs. Inclusion of the excitonic effect at an optically excited finite system within TDLDA is discussed in [18], while our current approach shows transient dynamics of photo-excited carriers within a short time. Examining the influence of the e–h bound state [20, 21] within such a short time is outside the scope of this paper.

The validation of the xc functional in the real-time propagation TDDFT scheme is not yet available, and we used LDA in the present study. However, for the ground-state properties, the performance of the LDA can be evaluated. For this purpose, we used the FHI-aims code[5]. We compared the binding energies and charge transfer properties of dimers from different theoretical approaches: LDA [11, 12, 22], generalized gradient approximation (GGA) [23] and hybrid functionals [24, 25]. GGA functionals [23] of a version of the Perdew, Burke and Emzerhof (PBE), revPBE, Becke–Lee–Yang–Parr (BLYP) functional and hybrid functionals [24, 25] of PBE0 and B3LYP were used. The van der Waals (vdW) correction approach (PBE+vdW) [26] (with C_6/R^6 tails, where C_6 coefficients are calculated from the self-consistent density), the van der Waals density functional (vdW-DF) [27] and MP2 results were compared.

There are two main issues with DFT xc functionals. (i) The dispersion interaction, important for stabilizing the donor–acceptor structures, is missing in the conventional xc. The large overbinding present in LDA calculations erroneously mimics the vdW attraction although the long-range dispersion interaction is missing in LDA. This leads to structures obtained with LDA that agree rather well with those derived from vdW corrected xc functionals, and therefore the structures optimized within LDA were kept. (ii) Self-interaction errors (SIE): transferred electrons between the molecules are spatially localized, where spurious charges are induced due to electron delocalization errors (or SIE) (see, e.g., [28]). We have looked into this problem very carefully for the case of TTF–TCNQ dimers (details can be found elsewhere [29]); spurious charges can be removed by including a certain portion of exact exchange. After the correction, the amount of transferred charges is reduced; consequently, the highest occupied molecular orbital and lowest unoccupied molecular orbital (HOMO–LUMO) gap increases. It would be desirable, of course, to have a kernel with correct dispersion interaction and SIE correction. There are ongoing efforts along these lines [30].

3. Ground-state properties

3.1. Structural properties

With respect to the dimer binding energy and the inter-molecular distance, experimental information is lacking. TTF–TCNQ forms a segregated phase [31, 32] of quasi-one-dimensional chains of donors and acceptors, which are arranged in a herringbone-like fashion. There are experimental data available on the cohesive energies of the segregated phase. The mixed form

[5] This is an all-electron electronic structure code using numerical atom-centered orbitals (NAO) as a basis set. We employed 'really tight' settings, including the standard NAO basis set 'tier2' for H, C, N and 'tier1' for S. For the Møller–Plesset perturbation theory (MP2), Hartree–Fock (HF) and hybrid functional calculations, counterpoise correction was performed for binding energy calculations and more basis functions were added to the 'tier3' level, which lead to total number of basis functions to 1580 and 7338 auxiliary wave functions. This choice of basis settings leads to a converged binding energy of the TTF–TCNQ dimer on the scale of meV.

is not the most favorable in the condensed phase, and there are no experimental data yet to compare with our theory. Within the GGA or hybrid functionals the interaction between the molecules is negligible, which reflects that vdW interactions are essential for describing the structural properties of these systems. The LDA is the only DFT functional that gives strong binding between the two molecules. The calculated results are: (0.92 eV, 3.19 Å) for the LDA, small binding for PBE (0.23 eV, 3.79 Å) and revPBE (0.14 eV, 4.59 Å), and hybrids (B3LYP of 0.13 eV, 4.0 Å). Using recent methods that include the van der Waals interaction, we obtain (0.79 eV, 3.40 Å) for PBE+vdW [26] and (0.66 eV, 3.64 Å) for vdW-DF [27] and (1.11 eV, 3.18 Å) for MP2. It is well known that vdW-DF gives too large distances for dimers [27] and MP2 overestimates vdW, and we put higher trust in the PBE+vdW results. For the MP2+ΔvdW approach [33], atomic C_6 coefficients from MP2 calculations are needed. To date, there have been no general approaches that have obtained those values for molecules; thus it is not feasible at this moment to get the precise values from this approach.

3.2. Ionization potential and electron affinity

The ionization potential (IP) of TTF and the electron affinity (EA) of TCNQ are closely related to the expected electron transfer of the dimer. The experimental results are 6.40 eV [34, 35] for the IP of TTF and 2.80 eV [36] for the EA of TCNQ. Our corresponding theoretical numbers, as calculated by the Δ self-consistent field (SCF) approach [18], are 6.29 (3.75) eV for LDA, 6.18 (3.56) eV for PBE, 6.14 (3.50) eV for revPBE, 6.33 (3.70) eV for B3LYP, 5.88 (3.12) eV for HF and 6.53 (2.98) eV for MP2. Here the first number is the IP of TTF and the number in parentheses is the EA of TCNQ. All of the values are obtained from the ground-state geometry of a given functional, and PBE+vdW geometries were taken for the MP2, HF and B3LYP calculations. These values are in good agreement with previous calculations [37–41]. The IP values from LDA and PBE calculations are reasonably close to the experimental data, while all the DFT results overestimate EA values. This is due to the SIE in the conventional DFT, where electron-delocalized states are spuriously overstabilized [28, 42].

Hirshfeld and Mulliken analyses agree on the total amount of transferred charge (ΔQ), with $\approx 0.4e$ using LDA ($0.38e$ for PBE, $0.32e$ for revPBE and $0.25e$ for B3LYP). Once spurious charges are removed, ΔQ decreases to $0.1e$ [29] (also see section 2). For a TTF–TCNQ crystal, neutron scattering measurements have shown that $0.59e$ are transferred in ambient condition and $0.616e$ as the pressure increases to 5 kbar [43]. The charge transfer between the molecules results in a finite electric field in the interlayer spacing of the molecular pair.

4. Excited state properties

4.1. Time-dependent density functional theory approach

The time evolution of the electronic structure was computed within the real-time TDDFT–molecular dynamics (MD) formalism, maintaining self-consistency between the wave function and the potential, both evolving in time [9, 10]. We used extremely short time steps of 1.94×10^{-3} fs to accurately describe the electron dynamics. These are three orders of magnitude shorter than those used in ground-state *ab initio* MD simulations of the nuclei dynamics. We found that ≈15 fs is a time scale which is long enough to monitor a significant change in the electron distribution (also see [44]).

We applied an external electric field (E-field) with polarization direction (x) depicted by the bold arrow in figure 1(a). The optical fields have excitation energies of 2.0 eV (620 nm) and 3.55 eV (349.3 nm), i.e. wavelengths that are ≈100 times larger than the size of the unit cell in the x-direction (the cell dimension was $16.7 \times 19.7 \times 17.8$ Å^3). Therefore, it is very reasonable to approximate the E-field by a spatially constant field while maintaining the sinusoidal ($\sin(\omega t)$) shape in time. We applied periodic boundary conditions and the field, generated from charged-dipole layers, becomes a periodic sawtooth-type modification of the external potential in space. The optical excitation is expressed by time modulation of the sawtooth-type potential. First of all, we applied a single pulse to compute the excitation energy within TDDFT by applying the Fourier transformation of the subsequent motion of the dipole moment $P(t)$ with respect to the time axis. We employed a Gaussian single shot with the full-width at half-maximum as 0.125 fs, which enables us to monitor the response of the system with excitation energies up to 5.26 eV, i.e. inverse of 0.125 fs, and the pulse has a maximum E-field strength of 0.3 V Å^{-1}. Although the pulse intensity does not affect the time constant of response, it affects the amplitude of $P(t)$. We have chosen the intensity of E-fields to be high enough to make a time variation of $P(t)$ numerically detectable without being destructive to the system. Our intensity is in the typical order of magnitude of those used in a scanning tunneling microscope, where the observed material does not get destroyed as well. We monitored the subsequent motion of the electron cloud, computed by the real-time TDDFT scheme, and evaluated the dipole moment $P(t)$ up to 11 fs. Figure 1(b) shows the optical absorption spectrum, which was obtained by taking Fourier transformation of $P(t)$: $P(\omega) = \int_0^T \mathrm{d}t\, P(t)\exp(\mathrm{i}\omega t)(1-\cos(2\pi t/T))/2$, where $P(\omega)$ is the Fourier component at frequency ω, and T denotes the simulated time range 11 fs. We adopted the Hanning window function [45], $(1-\cos(2\pi t/T))/2$, to perform the Fourier transformation with a finite time range.

The TDDFT spectrum was compared with the static LDA optical spectrum, which is computed as

$$\frac{1}{\pi}\mathrm{Im}\sum_{v,c}\frac{|\langle c|P_x|v\rangle|^2}{|E_c - E_v - \hbar\omega + \mathrm{i}\delta|},$$

where we use a broadening factor δ of 0.05 eV. This factor is necessary to avoid numerical instability. The current value of the broadening factor is sufficient to compare the feature of the excitation spectrum obtained by LDA and TDLDA. We found that LDA gives slightly lower excitation energies than those derived from TDLDA calculations. Similar behavior has been reported for many other studies [18]. To obtain well-converged values for the excitation energies by TDDFT, monitoring the dynamics of $P(t)$ in a longer time range might be necessary. Our purpose is to observe photo-induced e–h dissociation by photo-excitation, with a special focus on the excitation energies at resonance frequencies, i.e. 2.00 and 3.55 eV (see figure 1(b)).

Next, we applied an alternating E-field with frequencies of 2.0681 fs (2.00 eV) and 1.16 fs (3.55 eV). In our case, the e–h dissociation occurs due to the internal electrostatic field of the dimer, which means that the effect is independent of the applied field strength (only the required time for the dissociation is affected by the field strength). We chose the maximum intensity of the applied field as 0.07 V Å^{-1} and monitored e–h dynamics; this field strength is higher than the typical laser field, but not so strong as to destroy the molecule in a short time. We have chosen such a high intensity to monitor the behavior of the dipole within the available computing time. Energy conservation [46] under the presence of the time-varying E-field has been checked throughout the TDDFT-MD simulation. With the

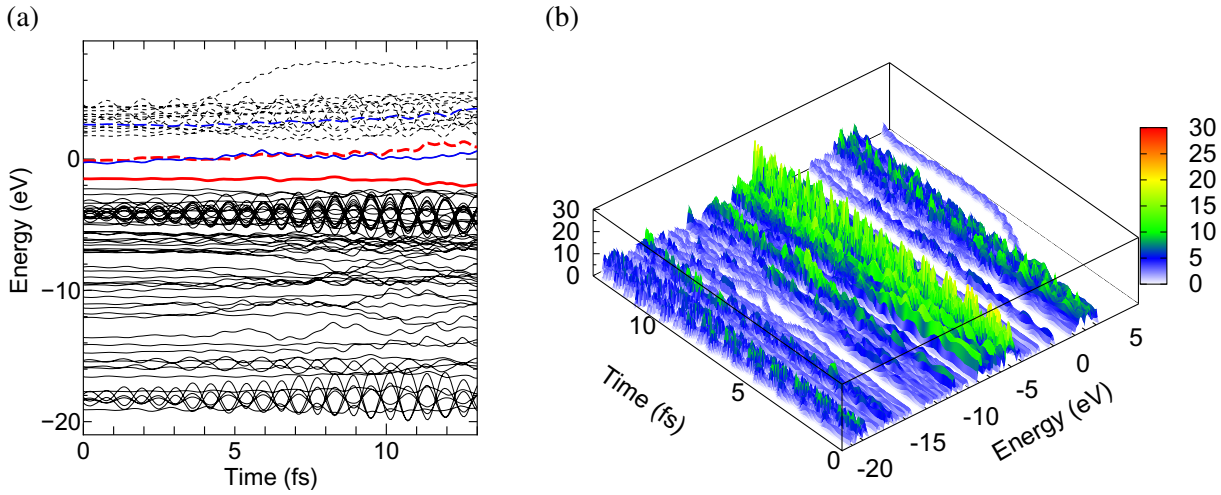

Figure 2. Time evolution of expectation values of the Kohn–Sham (KS) orbitals with an excitation energy of 3.55 eV (a) and their density of states (b), where a Gaussian broadening of 0.1 eV was used. Black solid and dashed lines are for occupied and empty molecular orbitals, respectively. Red (thick) solid and dashed lines are for the 61st and 63rd molecular orbitals, respectively, which are assigned as optical excitation pair according to the computed matrix element. Blue (thick) solid and dashed lines are for the 62nd and 68th molecular orbitals, respectively, which are also identified as optical excitation pair.

charge distribution determined by the time-evolving populated states, the Hellmann–Feynman forces were employed for the moving atoms [9, 10], which corresponds to the Ehrenfest approximation [47]. While there are no noticeable changes in their ionic configurations[6], we observe a growth of the Hellmann–Feynman forces of the order of $\approx 1.54\,\mathrm{eV\,\AA^{-1}}$ at several atomic sites when the excitation energy of light is 3.55 eV, which means that there will be an increase in electron–phonon coupling for a longer time. It will take a longer time scale to study exciton and polaron dynamics.

4.2. Electronic properties

Figure 2 shows the time evolution of the expectation values of KS orbitals with an excitation energy of 3.55 eV. Solid and dashed lines are for occupied and empty molecular orbitals, respectively. The HOMO and LUMO are depicted as a thick blue solid line and a thick red dashed line, respectively. The excitation pairs of the 61st (HOMO-1, thick red solid line) and the 63rd (LUMO, thick red dashed line), as well as the 62nd (HOMO, thick blue solid line) and the 68th (LUMO+5, thick blue dashed line) molecular orbitals, are identified as major optical excitation pairs by computing the transition matrix elements for the excitation energy of 3.55 eV. Predicting the correct sequence of populated levels is a challenging task, specifically

[6] The ions are 1836 times heavier than electrons; thus they start to move much later in the time scale. For example, assuming that a force of $1.54\,\mathrm{eV\,\AA^{-1}}$ is constantly applied to a C atom from the beginning of the molecular dynamics simulations, we obtain only a ≈ 0.1 Å displacement of the atom in 15 fs (using the classical Newton dynamics), i.e. even this overestimated value for the ionic displacement is negligible.

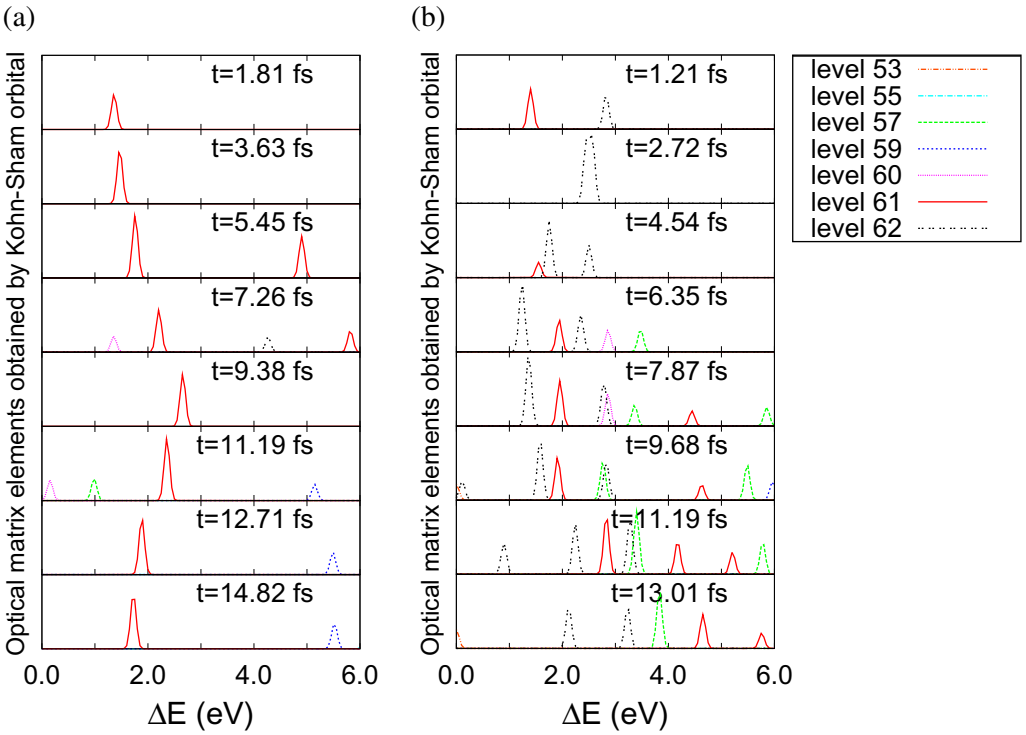

Figure 3. Time evolution of optical matrix elements of KS orbitals with excitation energies of 2.00 eV (a) and 3.55 eV (b). The contributions of matrices between levels i ($i = 53, 55, 57, 59, \ldots, 62$) and levels f ($f > 62$) were taken. The lateral axis (ΔE) is the difference in expectation value between levels i and f.

in the case of level alternation, which occurs in the single-electron spectrum following the electronic excitations. In particular, we observed strong level alternations for level 68 and for levels between 62 and 63. However, we found quite different characteristics for these crossing orbitals, and expect no non-radiative transition among adiabatic potential energy surfaces. This argument is quantified by monitoring the matrix elements of the KS Hamiltonian (H), including the optical E-field as a function of time, $|\langle f|H(t)|i\rangle|^2$; the matrix elements are related to the optical transition between the ith and the jth KS orbitals. The KS excitation energy (ΔE) shown in figure 3 is approximately on the scale of the optical excitation energy. In the beginning of the simulation, we observed many pairs of excitations, which will eventually merge to a single peak once the system reaches its equilibrium. The considered excitations correspond to the population of electrons from level i ($i = 53, 55, 57, 59, \ldots, 62$) to levels f located up to ≈ 6.0 eV higher than the location of levels i in expectation values under the excitation energy 2.00 eV (a) and 3.55 eV (b). Levels 62 and 63, which have almost degenerated at $t = 0$ (see figure 2), become split with the differences in the expectation values up to < 1 eV as evolved in time. However, we observed no significant off-diagonal matrix element between level 62 and those in the range of expectation value ≈ 1 eV under an optical excitation energy of 3.55 eV, as shown in figure 3(b). Thus the possible non-radiative transition between levels 62 and 63, for example, can be excluded within the time scale of ≈ 15 fs.

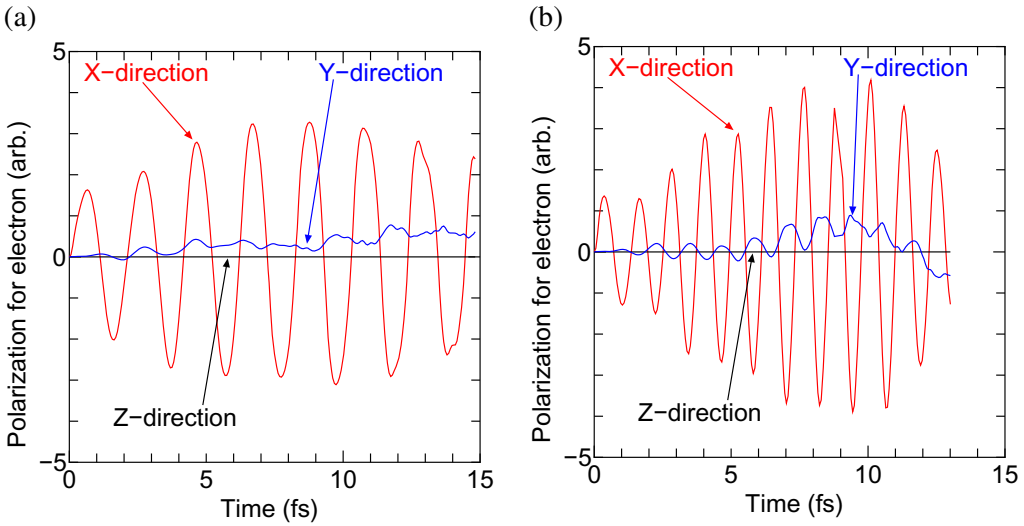

Figure 4. Time dependence of the change in polarization in the x-, y- and z-directions with respect to the values measured at $t = 0$ (a) with an excitation energy of 2.00 eV and (b) with an excitation energy of 3.55 eV.

Only a couple of excitations with energy below 2.00 or 3.55 eV are observed in the beginning. Then, the excited states evolve into a mixture of several pairs of excitations. For example, under excitation with 3.55 eV, the low-energy excitations ($\leqslant$3.0 eV) evolve in time to a distribution within an energy window 3.55 ± 2.0 eV. The peak heights evolved higher in the beginning of the simulation and were saturated. Meanwhile, the positions and the numbers of peaks change, indicating contributions of many excitation pairs to the electron dynamics. As time passes, the amount of increase in potential energy (total energy of the DFT) exceeds the optical excitation energy, indicating a possibility of multi-photon excitation[7].

4.3. Dipolar properties

The complicated nature of the response of the system to the external field is accompanied by non-trivial phenomena. One of them concerns the dipolar properties of the material, which are directly related to the behavior of electrons in the external field. To systematically investigate this phenomenon, we monitor the dynamics of the electron cloud with respect to the applied E-field, which varies in time as $E\sin(\omega t)$. In particular, we evaluate the time dependence of the vector of the dipole moment ($\mathbf{P}(t)$), which is defined as $\mathbf{P}(t) = \int(\mathbf{r} - \mathbf{r_0})n(\mathbf{r}, t)\mathrm{d}\mathbf{r}$, where $n(\mathbf{r}, t)$ is the electron density at position $\mathbf{r}$ and at time t, and $\mathbf{r_0}$ refers to a certain origin. Note that the time dependence of $\mathbf{P}(t)$ is independent of $\mathbf{r}_0$, since the total charge is constant with respect to time. We monitored the polarization in three directions: parallel (x-direction) and perpendicular (y- and z-direction) to the applied field. Figure 4 shows the time evolution of the polarization with respect to the values at $t = 0$, $\mathbf{P}(0)$, where the y-component value of $\mathbf{P}(0)$ is $\approx$60. The dipole moment increases by $\approx$1% for 15 fs, which is an indication of e–h dissociation. For the case with 3.55 eV excitation energy, we observed a slight decrease in the dipole moment at a later time. It is desirable to perform a large-scale simulation to understand

[7] Note that in the current approach, the classical E-field is used instead of the quantized photon.

the dissociation process. Eventually, we want to understand the mechanism of charge carrier transport of an extended system, which is more suitable for photovoltaic applications. It is, however, computationally very demanding to treat such a system. In a finite system, where no net charge can actually flow, the increase of local dipole moment has an analogy to the charge transport in an extended system.

The oscillation of the polarization of the direction parallel to the external field (x-direction) is due to the system's strong response to the external field. There are no changes in polarization in the z-direction, perpendicular to the external field. However, as the wave functions evolve in time we start to see a noticeable change in the y-direction at $t > 1$ fs. The overall increase and fluctuating behavior is similar to that in the x-direction, with $\approx 20\%$ of the amplitude. Such behavior was observed for the cases of both excitation energies, while polarization turns to decrease for excitation with 3.55 eV and remains enhanced for excitation with 2.00 eV. The enhancement of polarization occurs with satisfying total energy conservation; further increase in P_y is possible only through a photoemission process, which is outside the scope of this study.

An enhancement of the dipole moment in the direction parallel to the applied optical field was reported before [48], while the enhancement perpendicular to the applied optical field has not been reported as far as we know. This seemingly intriguing phenomenon stems from the strong distortion of the electronic character under photoexcitation, which further modifies the charge transfer behavior in time. Upon the formation of TTF–TCNQ dimer, there are significant changes in the electron density distribution of individual molecules; electrons are depleted over the TTF surface with high densities at π states of S and σ states of C in the middle of the carbon ring, while electrons are accumulated at the π states of N and C atoms of TCNQ. Figure 5 displays the electron densities, with respect to the density at $t = 0$.

N and S atoms are mainly responsible for the charge transfer properties of the pair, and their orbitals show a strong dynamic response to the applied optical field. In particular, an oscillation of the expectation values of σ and π states of N, S and C atoms is observed. In figure 2, the first oscillating region of expectation values near -19 eV corresponds to mostly N-σ orbitals, the next one near -16 eV corresponds to S-σ, and then near -4 eV the low-lying oscillating states are mostly from N-π, and the next one from C-π and S-π orbitals.

The strong response of S, N and C atomic states and their coupling to the external field induce additional charge transfer through their π and σ orbitals. In particular, additional electron accumulation or depletion between the molecules through their π orbitals, which are elongated perpendicular to the molecular plane, causes unexpected enhancement of their polarization direction perpendicular to the optical E-field. We monitored the evolution of the charge density in time. At $t = 0$, there is a charge accumulation (depletion) of $0.4e$ at the TCNQ (TTF) molecule. At $t = 9.378$ fs under an excitation energy of 3.55 eV, for example, additional charges of $\approx 0.15e$ are accumulated at TCNQ and depleted at the TTF molecule. On the other hand, at $t = 12.705$ fs, TCNQ loses its electrons by $\approx 0.10e$ compared to that of $t = 0$, which in turn decreases the polarization of the molecule in the y-direction. Figure 5 shows snapshots of the charge density (Δn) plot of these two time steps, where strong changes in y-polarization were observed. Here, Δn is defined as changes in charge density of the dimers obtained from TDLDA with respect to static LDA calculation ($t = 0$). The left panels show cross-sections cutting both TTF (bottom) and TCNQ (top) molecules at their central lines. The middle panels are cross-sections parallel to and 0.42 Å below the molecular plane of TCNQ. The right panels are cross-sections parallel to and 0.42 Å above the molecular plane of TTF. Red (thick) contour lines are for accumulated charges (electrons) and blue (thin) lines are for depleted charges (holes).

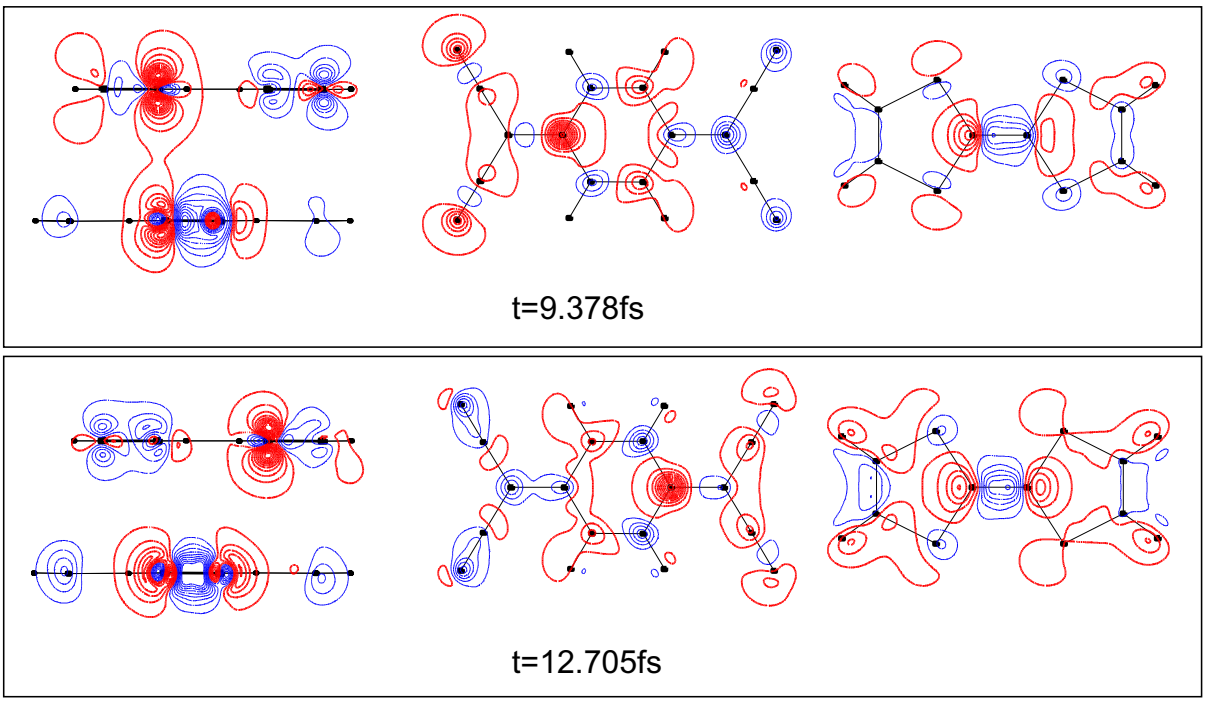

Figure 5. Variation of the charge density of TDLDA calculation compared with the static LDA calculation at $t = 9.378$ and 12.705 fs, with an excitation energy of 3.55 eV. The left panels show cross-sections cutting both TTF (bottom) and TCNQ (top) molecules at their center lines. The middle panels are cross-sections parallel to and 0.42 Å below the molecular plane of TCNQ. The right panels are cross-sections parallel to and 0.42 Å above the molecular plane of TTF. Red (thick) contour lines are for accumulated charge (electrons) and blue (thin) lines are for depleted charge (holes).

The modulation of the charge density along the x-axis simply follows the time-varying optical E-field, while that in the y-direction represents the behavior of polarization along the y-axis shown in figure 4(b).

5. Summary and conclusions

We theoretically studied the optical properties of TTF–TCNQ dimers, which are electron donor and acceptor pairs, using *ab initio* TDDFT. We found that our system shows very intriguing electronic properties when these are optically excited. The dipolar nature of the dimer changes dramatically under electronic excitation, and an unusual increase of the dipole moment of the system perpendicular to the applied electric field is observed. This is particularly because of the photo-induced electron transfer from donor to acceptor molecules through their π-orbital. The charge transfer is assisted by the finite E-field between TTF and TCNQ molecules even at the ground state. The photo-induced dipole enhancement is due to e–h dissociation that is a key component of photovoltaic phenomena. When we are able to make building blocks of p- and n-type layers by these molecules and proper electrodes at the end of the building blocks to extract photo-induced current, the photovoltaic performance of a layered organic material can be examined.

Acknowledgments

We acknowledge Professor A Rubio and Dr K H Kim for comments on this work. MY is sponsored by the US Department of Energy, Basic Energy Sciences, Materials Sciences and Engineering Division, the Laboratory Directed Research and Development Program of Oak Ridge National Laboratory, managed by UT-Battelle, LLC, for the US Department of Energy, and the Max Planck Society. YM acknowledges funding from the HPCI Strategic Program of MEXT.

References

[1] Walzer K, Maenning B, Pfeiffer M and Leo K 2007 *Chem. Rev.* **107** 1233
[2] Koch N 2007 *Chem. Phys. Chem.* **8** 1438
[3] Gershensen M E, Podzorov V and Morpurgo A F 2006 *Rev. Mod. Phys.* **78** 973
[4] Braga D and Horowitz G 2009 *Adv. Mat.* **21** 1473
[5] Bach U, Lupo D, Comte P, Moser J E, Weissortel F, Salbeck J, Spreitzer H and Gratzel M 1998 *Nature* **395** 583
[6] Peumans P, Yakimov Y and Forrest S R 2003 *J. Appl. Phys.* **93** 3693
[7] Hoppe H and Sariciftci N S 2004 *J. Mater. Res.* **19** 1924
[8] Runge E and Gross E K U 1984 *Phys. Rev. Lett.* **52** 997
[9] Sugino O and Miyamoto Y 1999 *Phys. Rev.* B **59** 2579
[10] Sugino O and Miyamoto Y 2002 *Phys. Rev.* B **66** 89901
[11] Ceperley D M and Alder B J 1980 *Phys. Rev. Lett.* **45** 566
[12] Perdew J P and Zunger A 1981 *Phys. Rev.* B **23** 5048
[13] Troullier N and Martins J L 1991 *Phys. Rev.* B **43** 1993
[14] Rohlfing M and Louie S G 2000 *Phys. Rev.* B **62** 4927
[15] Marques M, Ullrich C A, Nogueira F, Rubio A, Burke K and Gross E 2006 *Time Dependent Density Functional Theory (TDDFT)* (*Lecture Notes in Physics* vol 706) (Berlin: Springer)
[16] Castro A, Marques M, Varsano D, Sottile F and Rubio A 2009 *C. R. Phys.* **10** 469–90
[17] Varsano D, Marini A and Rubio A 2008 *Phys. Rev. Lett.* **101** 13302
[18] Onida G, Reining L and Rubio A 2002 *Rev. Mod. Phys.* **74** 601
[19] Hara K, Wang Z, Sato T, Furube A, Katoh R, Sugihara H, Dan-oh Y, Kasada C, Shinpo A and Suga S 2005 *J. Phys. Chem.* B **109** 15476
[20] Avalosab J, Devreux F, Guglielmia M and Nechtschein M 1978 *Mol. Phys.* **36** 669
[21] Styers-Barnett D, Ellison S, Mehl B, Westlake B, House R, Park C, Wise K and Papanikolas J 2008 *J. Phys. Chem.* C **112** 4507
[22] Perdew J P and Wang Y 1992 *Phys. Rev.* B **45** 13244
[23] Perdew J P, Burke K and Ernzerhof M 1997 *Phys. Rev. Lett.* **77** 3865
[24] Adamo C and Barone V 1999 *J. Chem. Phys.* **110** 6158
[25] Vosko S H, Wilk L and Nusair M 1980 *Can. J. Phys.* **58** 1200
[26] Tkatchenko A and Scheffler M 2009 *Phys. Rev. Lett.* **102** 073005
[27] Dion M, Rydberg H, Schröder E, Langreth D C and Lundqvist B I 2004 *Phys. Rev. Lett.* **92** 246401
[28] Cohen A J, Mori-Sánchez P and Yang W 2008 *Phys. Rev.* B **77** 115123
[29] Atalla V, Yoon M, Rinke P and Scheffler M in preparation
[30] Heßelmann A and Görling A 2011 *J. Chem. Phys.* **134** 034120
[31] Metzger R 1977 *J. Chem. Phys.* **66** 2525
[32] Langer J, Díez-Pérez I, Sanz F and Fraxedas J 2006 *Euro. Lett.* **74** 110
[33] Tkatchenko A, DiStasio R A Jr, Head-Gordon M and Scheffler M 2009 *J. Chem. Phys.* **131** 094106
[34] Seki N 1989 *Mol. Cryst. Liq. Cryst.* **171** 255–70

[35] Sato N, Saito G and Inokuchi H 1983 *Chem. Phys.* **76** 79
[36] Takendobu T, Takano T, Shiraishi M, Murakami Y, Ata M, Kataura H, Achiba Y and Iwasa Y 2003 *Nat. Mater.* **2** 683
[37] Milián B, Pou-Amérigo R, Viruela R and Ortí E 2004 *J. Mol. Struct. (Theo.)* **709** 97
[38] Ortí E, Viruela R and Viruela P M 1996 *J. Phys. Chem.* **100** 6138
[39] Demiralp E and Goddard W A III 1997 *J. Phys. Chem.* A **101** 8128
[40] Gahungu G, Zhang B and Zhang J 2006 *J. Phys. Chem.* B **100** 16852
[41] Katan C 1999 *J. Phys. Chem.* A **103** 1407
[42] Cohen A J, Mori-Sánchez P and Yang W 2008 *Science* **321** 792
[43] Megtert S, Comès R, Vettier C and Pynn R 1979 *Sol. Stat. Commum.* **31** 977
[44] Yabana K and Bertsch G F 1996 *Phys. Rev.* B **54** 4484
[45] Press W H, Teukolsky S A, Vetteling W T and Flannery B P 2007 *Numerical Recipes* 3rd edn (Cambridge: Cambridge University Press)
[46] Miyamoto Y and Zhang H 2008 *Phys. Rev.* B **77** 165123
[47] Ehrenfest P 1927 *Z. Phys.* **45** 455
[48] Miyamoto Y 2010 *Appl. Phys. Express* **3** 047202